Nuclear Instruments and Methods in Physics Research A 592 (2008) 456–462

Contents lists available at ScienceDirect

Nuclear Instruments and Methods in Physics Research A

journal homepage: www.elsevier.com/locate/nima

Implementation of the Legendre Transform for track segment reconstruction in drift tube chambers

T. Alexopoulos *, M. Bachtis, E. Gazis, G. Tsipolitis

Department of Physics, National Technical University of Athens, 9 Heroon Polytechniou Street, GR 157 80, Athens, Greece

ARTICLE INFO

Article history:
Received 26 March 2007
Received in revised form
28 March 2008
Accepted 15 April 2008
Available online 7 May 2008

Keywords:
Track reconstruction
Legendre transform
Slope transform
Drift tube chambers

ABSTRACT

In this study, we apply the geometrical properties of the Legendre transform in order to implement a segment reconstruction algorithm for drift tube chambers used in High Energy Physics experiments. The output signal of a drift tube chamber consists of a collection of circles, each of which corresponds to a drift tube and defines the trajectory of the charged particle. The particle track candidate is reconstructed as the common tangent line to the drift circles. We tested the method both on an ideal case and on a case of high noise conditions using Monte Carlo generated tracks.

1. The Legendre transform

The Legendre transform [1,2] is a well-known mathematical tool in Thermodynamics and Analytical Mechanics. Consider a convex function $f:\mathscr{R}\rightarrow\mathscr{R}$ ($\mathrm{d}^2f/\mathrm{d}x^2>0$) and a straight line of the form $y=px+a$, where p and a are the slope and intercept, respectively. For a value p of the slope the Legendre transform $F(p)$ of the function $f(x)$ is defined as follows [1,2]

$$F(p)=\sup_x[px-f(x)]=-\inf_x[f(x)-px]$$

The notation $\sup_x$ indicates the maximization of the function $px-f(x)$ with respect to x for constant p, while $\inf_x$ indicates the minimization of $f(x)-px$ with respect to x for constant p. The relationship between $f(x)$ and its Legendre transform is denoted by

$$f(x)\overset{\mathscr{L}}{\longleftrightarrow}F(p)$$

As it is demonstrated in Fig. 1a, for a given value p of the slope, this transform finds the point of $f(x)$, where the tangent line has a slope p. The intersection of the straight line with the y-axis is given by $-F(p)$. Thus, each point $(p,F(p))$ in Legendre space represents a line, tangent to the curve $f(x)$. The Legendre transform can also be applied to a concave function (Fig. 1b) where $\mathrm{d}^2f/\mathrm{d}x^2<0$, by defining it as

$$F(p)=\sup_x[f(x)-px]=-\inf_x[px-f(x)]$$

where the intersections of the tangent lines is given by $F(p)$.

Thus, the Legendre transform can be applied to any type of functions, either convex or concave. This property leads to the idea of generalizing the Legendre transform by introducing the "Slope" transform [3] for any kind of function.

The Legendre transform of a convex function $f(x)$ at a point x_0 can be constructed with the following two equations:

$$p=\left.\frac{\mathrm{d}f}{\mathrm{d}x}\right|_{x=x_0} \quad (1)$$

$$F(p)=px_0-f(x_0) \quad (2)$$

If x_0 is expressed as a function of p using Eq. (1) and the result is inserted into Eq. (2), the resulting expression, $F(p)$, is only a function of p.

To illustrate the method of constructing the Legendre transform of a function, we compute the Legendre transform of a simple function, $f(x)=x^2/2$, as an example. In this case, $p=\mathrm{d}f/\mathrm{d}x=x$, therefore the Legendre transform is expressed as

$$F(p)=px-f(x)=p^2/2\Rightarrow x^2/2\overset{\mathscr{L}}{\longleftrightarrow}p^2/2$$

so, a parabola becomes a parabola in Legendre space.

Table 1 lists the Legendre transform of some common functions. Note that the functions $x^3/3$ and $-1/x$, include both a convex and a concave part.

Some of the interesting properties of the Legendre transform are summarized in Table 2. In this table, $f(x)\overset{\mathscr{L}}{\longleftrightarrow}F(p)$ and $g(x)\overset{\mathscr{L}}{\longleftrightarrow}G(p)$ represent the Legendre transforms.

* Corresponding author. Tel.: +30 210 7723019; fax: +30 210 7723021.
E-mail address: Theodoros.Alexopoulos@cern.ch (T. Alexopoulos).

0168-9002/$ - see front matter
doi:10.1016/j.nima.2008.04.038

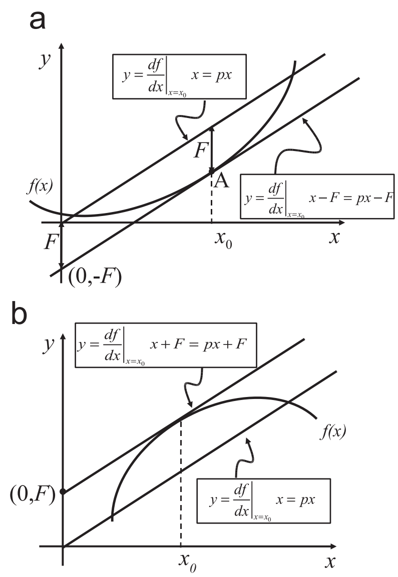

Fig. 1. The Legendre transform corresponding (a) to a convex and (b) to a concave function.

Table 1
The Legendre transform of some common functions

Original function	Legendre transform
$x^2/2$	$p^2/2$
e^x	$p(\ln p - 1)$
$\ln x$	$-\ln(ep)$
x^a/a	p^b/b where $1/b + 1/a = 1$
$x^3/3$	$(2/3)p^{3/2}$
$-1/x$	$-2p^{1/2}$

Table 2
Properties of the Legendre transform

Property	Result
Scaling	$af(x) \overset{\mathscr{L}}{\longleftrightarrow} aF(p/a)$
Stretching	$f(ax) \overset{\mathscr{L}}{\longleftrightarrow} F(p/a)$
Translation	$f(x-a) \overset{\mathscr{L}}{\longleftrightarrow} F(p) + a$
Linear addition	$f(x) + ax + b \overset{\mathscr{L}}{\longleftrightarrow} F(p-a) + b$
Young's inequality	$px \leqslant f(x) + F(p)$
If $f(0) = \mathrm{d}f/\mathrm{d}x\|_{x=0} = 0$	$F(p) = \int_0^p (\mathrm{d}f/\mathrm{d}x)^{-1}\,\mathrm{d}x$
Infimal convolution $(f \oplus g)(x)$ $= \inf_y \{f(x-y) + g(y)\}$	$(f \oplus g)(x) \overset{\mathscr{L}}{\longleftrightarrow} F(p) + G(p)$

The $(\mathrm{d}f/\mathrm{d}x)^{-1}$ denotes the inverse function of the first derivative $\mathrm{d}f(x)/\mathrm{d}x$.

2. Description of the method

In the following we shall apply the Legendre transform to the drift tube chambers of the ATLAS experiment [4,5]. The chambers consist of layers of drift tubes filled with a gas mixture. Each drift tube is constructed with a grounded metallic cathode cylinder and an anode wire, passing through its center, held at a positive potential. A charged particle passing through the tube ionizes the gas along its path. The resulting electron avalanche travels towards the wire, while the produced ions drift towards the cathode cylinder, generating a trigger pulse that is detected by the detector electronics. The drift time is the time span between the trigger pulse and the anode wire pulse. A calibration formula relates the drift time of the electrons to the distance of the particle path from the anode wire. Each drift tube signal is depicted as a circle, concentric with the tube. The circles represent all the possible track paths that cross the chamber. Each particle track is the common tangent that can be drawn to a collection of circles from several layers (Fig. 2a). Several algorithms have been used to solve this kind of problem [6–9].

2.1. Transformation into Legendre space

In this article a new algorithm, based on the Legendre transform, will be described. The implementation of the Legendre transform for finding tracks is based on the transform of each drift circle to the Legendre space. The point with the maximum contribution, in the Legendre space, represents the common tangent to the circles. A circle can be defined by a combination of a convex and a concave function as shown in Fig. 2b. The equation of a circle with center (x_0, y_0) and radius R is given by

$$f(x) = \begin{cases} f_1(x) = y_0 + \sqrt{R^2 - (x - x_0)^2} \\ f_2(x) = y_0 - \sqrt{R^2 - (x - x_0)^2} \end{cases}$$

where equation $f_1(x)$ refers to the concave part and $f_2(x)$ to the convex part, respectively. In the concave case, the Legendre transform is

$$F_1(p) = \sup_x [f_1(x) - px], \quad p = \frac{\mathrm{d}f_1}{\mathrm{d}x}$$

The first derivative $p = \mathrm{d}f_1/\mathrm{d}x$ is

$$p = -\frac{x - x_0}{\sqrt{R^2 - (x - x_0)^2}} \Rightarrow x = x_0 \frac{|p|R}{\sqrt{p^2 + 1}}$$

For the concave case, the minus sign is as it should be, because for $x > x_0$, $p < 0$ and for $x < x_0$, $p > 0$ (Fig. 3b), so $x = x_0 - pR/\sqrt{p^2 + 1}$ is used for the Legendre transform which is

$$F_1(p) = f_1(x) - px = y_0 - x_0 p + R\sqrt{p^2 + 1}$$

so the circle is transformed to a hyperbola in Legendre space.

As mentioned above, each pair $(p, F(p))$ defines a tangent to the circle. For normal behavior at large values of p, it is more suitable to express the line equation by its canonical form $r = x\cos\theta + y\sin\theta$ (Fig. 3a), so $p = -\cot\theta$ and $F(p) = r/\sin\theta$. In this case, the Legendre transform becomes

$$\frac{r}{\sin\theta} = y_0 + x_0 \frac{\cos\theta}{\sin\theta} + \frac{R}{\sin\theta}$$

$$\Rightarrow r = x_0 \cos\theta + y_0 \sin\theta + R = r_0 \cos(\theta - \phi) + R \quad (3)$$

where $r_0 = (x_0^2 + y_0^2)^{1/2}$, and $\phi = \arctan(y_0/x_0)$. This equation represents a sinogram in the r, θ Legendre transformation space as shown in Fig. 2c. Following the same calculation steps for the convex case, it can be shown that the Legendre transform has the form

$$F_2(p) = x_0 p - y_0 + R\sqrt{p^2 + 1}$$

and similarly, in the (r, θ) representation has the form

$$r = x_0 \cos\theta + y_0 \sin\theta - R = r_0 \cos(\theta - \phi) - R \quad (4)$$

Therefore, using Eqs. (3) and (4) the Legendre transform of the circle is reduced to

$$f(x) \overset{\mathscr{L}}{\longleftrightarrow} \begin{cases} r = x_0 \cos\theta + y_0 \sin\theta + R & \text{for concave} \\ r = x_0 \cos\theta + y_0 \sin\theta - R & \text{for convex} \end{cases} \quad (5)$$

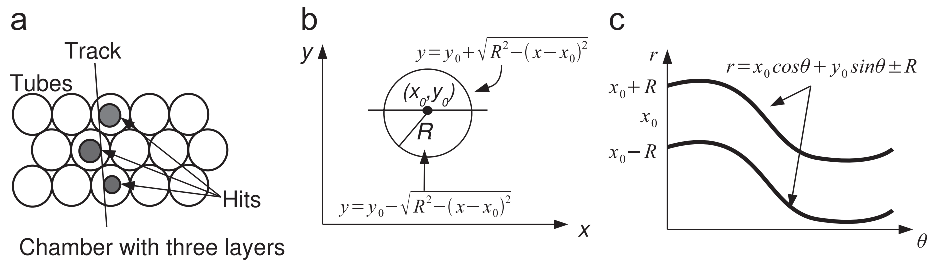

Fig. 2. (a) Drift circles and track in a Drift Tube Chamber, (b) Representation of the circle by a convex and a concave function, (c) Representation of the circle in Legendre transformation space. The circle corresponds to two sinograms in the Legendre transformation space.

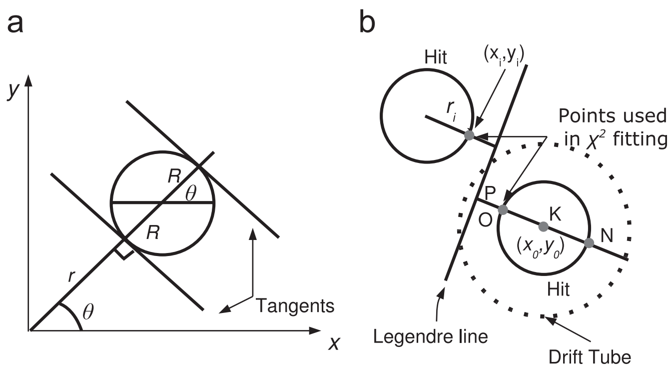

Fig. 3. (a) Tangent line in (r, θ) representation. (b) Selection of the points used in the χ^2 test.

It is worth mentioning that when the circle reduces to a point, in the limit of $R \to 0$, the Legendre transform is reduced to the Radon/Hough transform [2,10] of the point (x_0, y_0), providing us with a single sinogram in the (r, θ) space. In this case, the Legendre transform represents all the possible lines going through the point (x_0, y_0). Therefore, this technique could be used to reconstruct straight lines from a given set of points.

The input to the algorithm consists of the positions of the center of the drift circles and their radii. Taking into account the error of the measurement of the drift distance (radius) δR and the chosen step $\delta\theta$, while filling the histogram in Legendre space, it is found that the error of the line parameter r is

$$\delta r = \sqrt{\left(\frac{\partial r}{\partial R}\delta R\right)^2 + \left(\frac{\partial r}{\partial \theta}\delta\theta\right)^2}$$

$$\Rightarrow \delta r = \sqrt{\delta R^2 + (x_0 \sin\theta - y_0\cos\theta)^2 \delta\theta^2} \tag{6}$$

The error on the line parameter r consists of the angle step $\delta\theta$, of the drift distance error, δR , and of the hit position (x_0, y_0). In constructing the histogram, it is advantageous to choose a uniform binning, independent of the hit position. For this purpose, the angle step is selected to be $\delta\theta = 5 \times 10^{-4}$ rad, so that $\delta r \approx \delta R$. Moreover, to stay within a maximum drift error of 100 μm, the width of the r bin can be selected to the higher value of 200 μm, so that the error is included in the same bin of the histogram. This is very important because the transform takes into account all the drift circles that contribute to the line even if, due to the errors, the reconstructed line is not the actual tangent line. Moreover, considering the peaks in Legendre space, we notice an equality in the sense that the height of the peaks represents the number of circles that contribute to the charged particle track, something that will be used in the next reconstruction steps.

2.2. Clustering and extraction of lines

In transforming to the Legendre space, clusters of maxima are created in the two-dimensional histogram. The clusters are created due to the quantization of space that results from the selected binning. Therefore, a clustering algorithm is needed that will extract the peaks from the histogram. The search for clusters is facilitated by applying a threshold to the bins of the histogram. All bins that are under a specified threshold are ignored. This threshold depends on the reconstruction requirements. Due to the above procedure, this threshold is the minimum number of circles that are chosen to define a peak. For a maximum reconstruction efficiency, this threshold was chosen to be equal to 3 due to the fact that a minimum of three circles is required to define a common tangent line. Tighter cuts with thresholds of 4 or 6 circles per line may also be applied. After applying the appropriate threshold, the peaks are sorted by height and the neighboring bins of each peak are tested in an iterative process which results in clusters having the Legendre peaks as centers (Fig. 4a). The neighboring bins are labeled according to their height. We consider three cases in clustering the bins:

- The height of a neighboring bin is lower than the height of the central bin.
- The height of a neighboring bin is equal to the height of the central bin and the bins are adjacent to each other.
- The height of a neighboring bin is equal to the height of the central bin but there are smaller peaks between them.

In the first case the neighboring bin is dropped because it corresponds to a subset of the real segment. This line segment contains some of the real hits that belong to the actual line (Fig. 4b). In the second case there is a maximum next to the original maximum, therefore, it belongs to the same line. This bin is also ignored since this line has been already taken into account. Finally, in the third case, there is one more maximum but in a significant distance from the center bin (main tangent line). This means that there is a line that has different parameters from the central bin line but it is associated to the same number of circles. This bin is accepted because it might correspond to an ambiguous line. Ambiguous lines are lines that share the same hits but have different parameters (Fig. 4c). They are usually caused by some symmetrical sets of drift circles. The clustering for each maximum terminates at the last neighboring bin that has a height over threshold. The output of the clustering algorithms includes both the locally separated maxima and the bins that correspond to possible ambiguous lines. This algorithm works for multi-track events as well, because the different tracks are separated in space so the maxima are also separated in Legendre space. It is noted that in a drift tube chamber, it is not possible for two tracks to

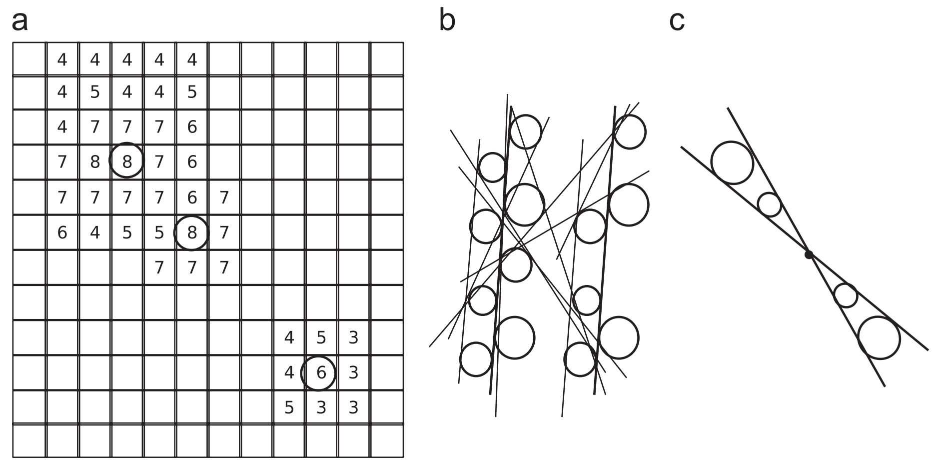

Fig. 4. (a) Clusters on the Legendre histogram after the threshold cuts (b) Line and neighboring subset lines that need to be dropped. (c) Ambiguous lines that are associated to the same circles but they have different line parameters.

share the same hits, since only the earliest (nearest to the anode wire) signal will be accepted for an event.

2.3. Least squares fit

After identifying the lines in the Legendre histogram, the various drift circles are been associated with the lines. The criterion used for associating a circle with a line is

$$|d_i - r_i| < 5\sigma$$

where d_i is the shortest distance between the center of the drift circle and the line, r_i is the radius of the circle and σ is the error of the drift radius that is known from the fit of the calibration "r, t" relation. After this association procedure, a least squares fit is applied to extract the line parameters with high accuracy. Depending on the required precision of the measurement, an analytical least squares method was used. For this fit, a series of points belonging to the hit circles and having the minimum distance from the Legendre calculated line are used (Fig. 3b). For the calculation of the points that will contribute to the least squares fit, it is assumed that the transform reconstructed line has the form $y = \alpha x + \beta$. Let r_i define the radius of the circle (hit) and (x_0, y_0) the center of the tube. The coordinates of the points O, N that belong to the track, Fig. 3b, can be calculated using the equations

$$x_i = x_0 \frac{r_i}{\sqrt{\alpha^2 + 1}}, \quad y_i = y_0 \mp \frac{1}{\alpha} \frac{r_i}{\sqrt{\alpha^2 + 1}}$$

The point with the minimum distance from the reconstructed line (in this example, the point is represented by O) is selected for the least squares fit.

3. Performance study

In order to study the proposed method, a Monte Carlo algorithm is used to produce random lines and create the hits for each tube. As an example, the algorithm is tested in the new Monitored Drift Tube detector of the ATLAS experiment, a straw type chamber, currently under commissioning. In this study, a Drift Chamber of eight tube layers including 36 tubes in each layer, is used. The diameter of each tube is 30 mm. After calculating the hits, a Gaussian measurement error is applied to each hit. Moreover, random hits are generated to simulate random noise hits in the detector. The study is performed for single and multi-track events. In each case, the reconstructed line parameters are calculated. It is worth mentioning that in the ATLAS experiment the main source of noise hits comes from low-momentum tracks. The noise hits from these tracks will probably affect the reconstruction of the high momentum tracks in a significantly different way than the randomly distributed noise hits. This kind of study will be addressed in a future work.

3.1. Resolution

For a quantitative evaluation of the algorithm resolution in both clean and noisy events, suitable parameters are introduced. These parameters are the slope $\tan\theta$ and the offset x_0. (The function $y = (x - x_0)\tan\theta$, is the line parameterization, where $-x_0 \tan\theta$ is the intercept.) The residuals (see Fig. 3b) between the Monte Carlo drift radii and the radii as reconstructed for each hit after applying the proposed method, are also calculated as a global indicator of the resolution of the tracking algorithm.

Single track events are generated with random angles θ and offset x_0 from a source that is located 1 m away from the detector. The events are reconstructed with the method described above and the reconstructed values are compared to the original Monte Carlo values. The algorithm has been studied in a standard loose-cut configuration with a minimum threshold of three drift circles per line. Fig. 5 shows the results for single track events. Histograms (a)–(c) in Fig. 5 show the differences in slope $\tan\theta$, offset x_0, and residuals between the Monte Carlo and the reconstructed events. In this case no measurement error was applied to the hits. The residual error (resolution, which represents the intrinsic performance of the method) is $7.80 \pm 0.07\,\mu$m. The next three histograms (d)–(f) show the same parameters. A Gaussian measurement error with a standard deviation of 100 μm was applied to each hit. The resolution, $88.09 \pm 0.50\,\mu$m as shown in histogram 5(f), is close to the Gaussian measurement error with a standard deviation of 100 μm. Histogram 5(h) shows the residual error versus the Gaussian measurement error for a standard deviation of up to 500 μm. As demonstrated by this histogram, the method is stable providing a resolution compatible with the Gaussian measurement error. In the next step, randomly distributed hits with random radii, up to the radius of the tube, are generated in order to simulate the effect of noise on the system. In the case of multi-hits in a tube, the hit with the smaller radius (earlier hit) is taken into account because the readout detector electronics ignore all the later hits.

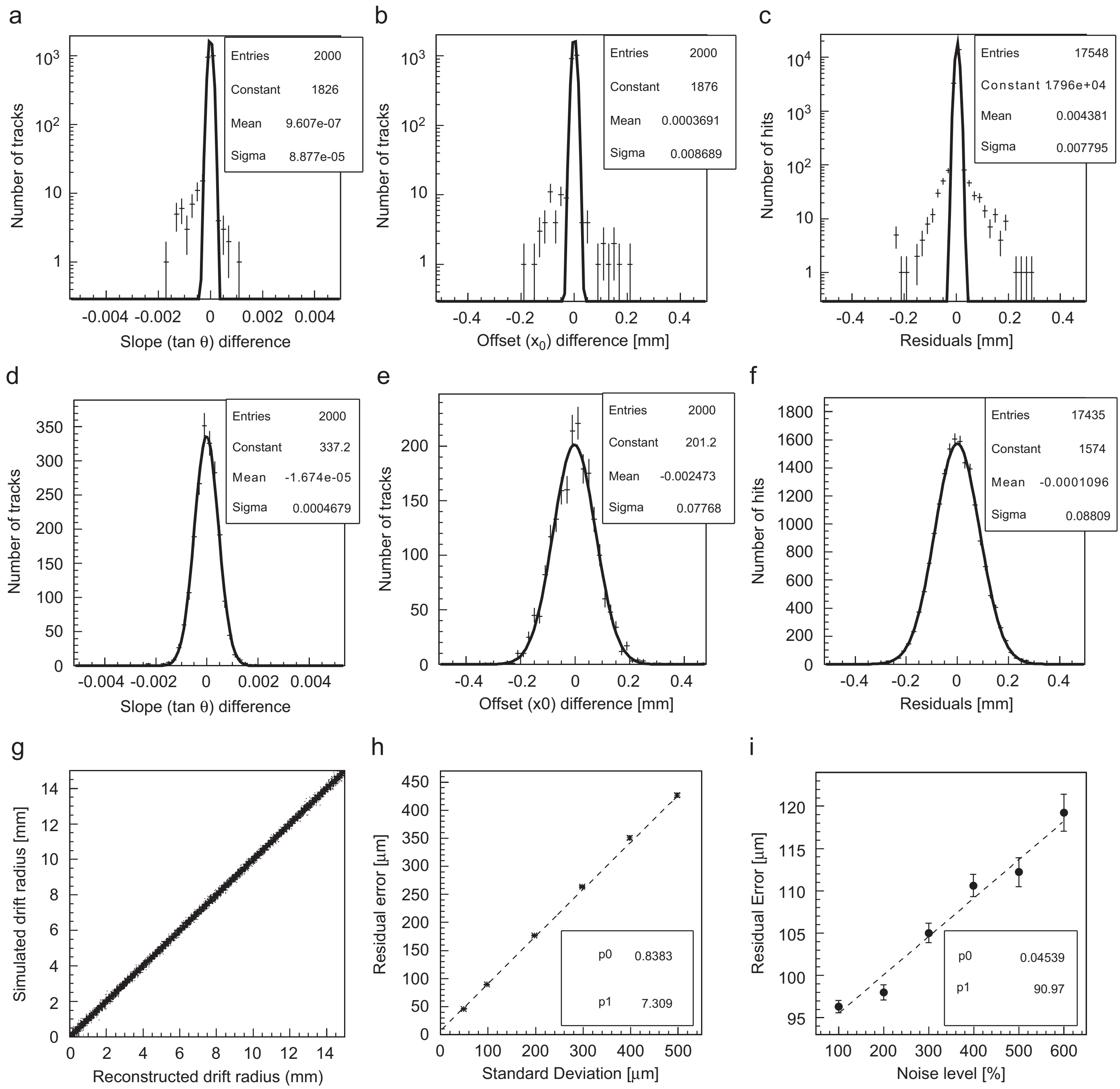

Fig. 5. Performance results for single track events. Histograms (a)–(c) display the difference of the Monte Carlo and the reconstructed events of slope angle, offset, and residuals, respectively. The residual error (resolution of the track reconstruction) is $3.26 \pm 0.03\,\mu$m. The next three histograms (d)–(f) show the same parameters with an applied standard deviation of $100\,\mu$m to each hit. The standard deviation of the fit in histogram (f) is $88.09 \pm 0.50\,\mu$m. Graph (g), is a plot of the correlation between the Monte Carlo generated radii and the reconstructed ones with a standard deviation of $100\,\mu$m. Graph (h) is a plot of the residual error in μm versus the standard deviation in μm, for a standard deviation up to $500\,\mu$m. Finally, in graph (i), we plot the resolution versus noise using hits with a standard deviation of $100\,\mu$m. The data are simulated with noise up to 600%.

The graph 5(i) displays the resolution versus noise. Data are simulated with extra noise hits up to 600% and with a Gaussian measurement error with a standard deviation of $100\,\mu$m applied to each hit. The method seems to be robust in noisy environments and could be very efficient in reconstructing tracks for chambers installed near the beam line of an experiment, where obviously the noise level is higher. Finally, diagram 5(g) displays a very good correlation between the Monte Carlo hit radii and the reconstructed ones displaying a Gaussian measurement error with a standard deviation of $100\,\mu$m.

3.2. *Reconstruction efficiency and fake rate*

Reconstruction efficiency and fake rate parameters of the algorithm are introduced for a better evaluation of its performance. The reconstruction efficiency is defined as

$$\text{Efficiency} = \frac{N_{\text{match}}}{N_{\text{sim}}}$$

where N_{match} and N_{sim} are the number of matched segments and simulated track segments, respectively. The fake rate is

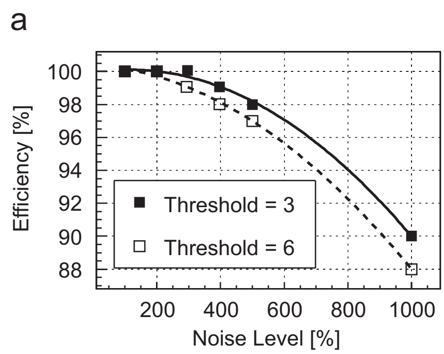

Fig. 6. Reconstruction efficiency and fake rate of the algorithm as a function of the Noise level for two different threshold configurations.

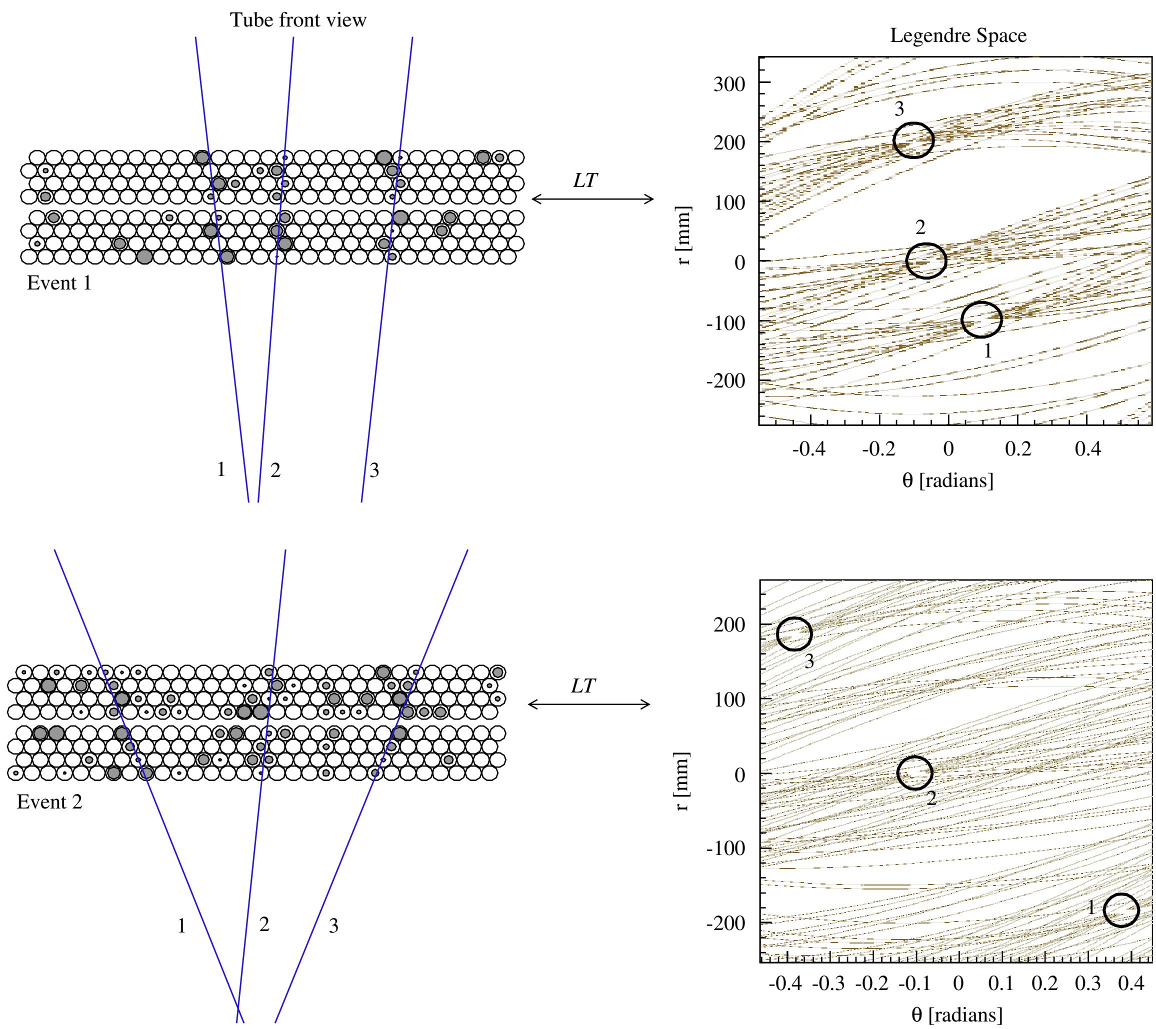

Fig. 7. Drift chamber with two multi-track events with noise level of 50% and 200%, for Events 1 and 2, respectively. Each one of the events were reconstructed using the Legendre transform method with their corresponding Legendre transforms. The circles in Legendre space graphs denote the points with the highest height, corresponding to the reconstructed tracks shown on the left graphs.

given by

$$\text{Fake Rate} = \frac{N_{\text{fakes}}}{N_{\text{sim}}}$$

where N_{fakes} are the reconstructed segments that were not matched to a simulated track (fake segments). The evaluation of the track match introduces the need for a matching criterion. A reconstructed line of the form $y = \tan\theta_1 x + b_1$ is matched to a simulated line of the form $y = \tan\theta_2 x + b_2$ if

$$|\theta_2 - \theta_1| < 0.01\,\text{rad} \quad \text{and} \quad |b_2 - b_1| < 0.1\,\text{mm}$$

Single track events are generated for different noise parameters and the reconstruction efficiency and fake rate are evaluated. The algorithm is used in two different configurations with a threshold of three and six drift circles per line, respectively. The results are presented in Fig. 6. The Legendre algorithm shows very high

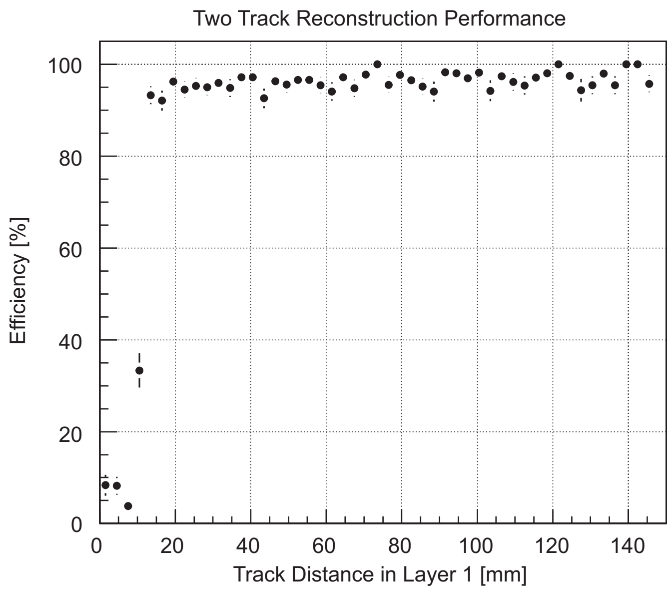

Fig. 8. Two-track efficiency versus track distance separation at the first layer (closest to the source) of the Drift Chamber.

reconstruction efficiency which is kept over 90% for all different noise levels (Fig. 6a). The reconstruction efficiency is slightly lower (by almost 2%) for the tight-cut configuration of minimum six drift circles per track. For the loose-cut configuration (three circles) the fake rate increases significantly as the noise level is increased (Fig. 6b). This is not surprising because in a very noisy environment a large number of lines with three random drift circles can be found. In noisy conditions it is wise to increase the threshold to clean up the signal. It is observed that for a threshold of six drift circles per line, the fake rate is lowered significantly, something that makes the Legendre algorithm a valuable tool for pattern recognition. Finally, Fig. 7 shows two reconstruction examples of multi-track events (three tracks in each event with 50% and 200% of extra noise hits, respectively), and the corresponding Legendre transform spaces. From this figure, it is evident that the Legendre transform segment reconstruction algorithm which we have used in this analysis is able to correctly reconstruct tracks in a noisy environment.

Furthermore, a two-track separation study was carried out by generating two-track events in the absence of noise hits. The two tracks of each event are originated from a common source that is located 1 m away from the Drift Chamber and they are propagated through a Drift Chamber of eight tube layers as shown in Fig. 7. The events are reconstructed using the Legendre transform method. It is clear that for two adjacent tracks, either one will lose some of its hits to the other track and reconstruction efficiency will suffer. The outcome of this study is summarized in Fig. 8. We observe that in the case of the two-track events the reconstruction efficiency of this algorithm is dropping for two tracks that are separated by a distance of less than 12.5 mm which is smaller than the radius (15 mm) of a singe tube.

4. Conclusion

A new efficient fast tracking method using the Legendre transform of circles in combination with a least squares fit has been developed. This method is successfully applied to a set of hits in a drift chamber using Monte Carlo simulated data. In the limit of zero radius of the circles, the Legendre transform is reduced to the Radon/Hough transform of a set of points providing us with an efficient method of tracking.

We intend to continue this work by integrating this algorithm into the ATLAS experiment muon spectrometer code in order to compare its reconstruction efficiency and fake rate with the other available algorithms.

Acknowledgments

We wish to thank the reviewer for the valuable comments and our colleague Emeritus Professor Anastasios Filippas for helpful discussions during the analysis of this work.

This work has been done in the framework of the Greek Ministry of Education project "PYTHAGORAS II" which is co-funded by the European Social Fund (75%) and National Resources (25%).

References

[1] V.I. Arnold, Mathematical Methods of Classical Mechanics, Springer, Berlin, 1989.
[2] T. Alexopoulos, Introduction to signal analysis, NTUA, 2004 (in Greek).
[3] L. Dorst, R. Van den Boomgaard, Signal Process. 38 (1994) 79.
[4] ATLAS Collaboration, Muon Spectrometer, Technical Design Report, CERN/LHCC/97-22, ATLAS TDR 10, 1997.
[5] T. Alexopoulos, et al., Nucl. Instr. and Meth. A 560 (2006) 633.
[6] D. Adams, et al., Track reconstruction in the ATLAS Muon Spectrometer with MOORE, ATL-SOFT-2003-007, ATL-COM-MUON-2003-012.
[7] M. Virchaux, Muonbox: a full 3D tracking programme for Muon reconstruction in the Atlas Spectrometer, ATL-MUON-1997-198.
[8] N.V. Eldik, The ATLAS muon spectrometer calibration and pattern recognition, PhD Thesis, University of Amsterdam, 2007.
[9] D. Primor, et al., A novel approach to track finding in a drift tube chamber, 2007 JINST 2 P01009.
[10] P.V.C. Hough, Method and means of recognizing complex patterns, U.S Patent 3,069,654. December 1962.